Pergamon

Int. J. Heat Mass Transfer. Vol. 37, Suppl. 1, pp. 457–463, 1994
Elsevier Science Ltd
Printed in Great Britain.
0017–9310/94 $6.00+0.00

0017–9310(93)E0111–S

Effect of fin efficiency on a model for condensation heat transfer on a horizontal, integral-fin tube

A. BRIGGS and J. W. ROSE

Department of Mechanical Engineering, Queen Mary and Westfield College, University of London, Mile End Road, London E1 4NS, U.K.

Abstract—A semi-empirical model for condensation on horizontal, integral-fin tubes has been adapted to account for 'fin efficiency effects'. Specimen calculations have been made to investigate the effect of tube geometry and material on the enhancement ratio for condensation of steam and CFC11. The best fin spacing was found to be only weakly dependent on the other geometric variables and fin thermal conductivity. The best fin thickness was more strongly dependent on fin thermal conductivity. For the refrigerant the optimum fin thickness was smaller than presently used in practice. The model gave satisfactory agreement with experimental data for CFC113 and steam for typical fin geometries. In the case of CFC113 the enhancement ratio was almost independent of fin thermal conductivity for conductivities exceeding around 50 W m^{-1} K^{-1}.

INTRODUCTION

A SIMPLE, semi-empirical equation for condensation on horizontal, integral-fin tubes with fins of rectangular cross-section has been obtained [1] and extended [2] to trapezoidal cross-section fins. The model combined the Nusselt [3] approach for gravity-drained condensation on vertical plates and horizontal tubes with dimensional analysis to account for the effects of surface tension on the condensate flow. The resulting equation was in good agreement with experimental data for various fluids from 19 investigations for condensation on copper tubes. Good predictions were obtained for optimum spacing between fins for given fin height, thickness and tube diameter. Since conduction in the fin was neglected (the whole of the fin was assumed to be at the fin root temperature) the model would be expected to become less accurate and to overestimate the 'enhancement ratio' with increasing values of $(\alpha h^2/tk_w)$. The present paper describes how 'fin-efficiency effects' can be incorporated into the model in an approximate way.

ANALYSIS

For rectangular-section fins, Rose [1, 2] gave expressions for the heat flux to the fin tip, fin flank and fin root. Dropping the assumption, made in the earlier work, of negligible temperature gradient in the fin, these equations can be rewritten as follows:

For the fin tip

$$q_{\text{tip}} = \left\{\frac{\rho h_{\text{fg}}}{\mu}(k\Delta T_{\text{tip}})^3\left[0.281\left(\frac{\tilde{\rho}g}{d_0}\right)+B_{\text{tip}}\left(\frac{\sigma}{t^3}\right)\right]\right\}^{1/4} \tag{1}$$

where B_{tip} is a dimensionless constant.

For the fin flanks

$$q_{\text{flank}} = \left\{\frac{\rho h_{\text{fg}}}{\mu}(k\overline{\Delta T}_{\text{flank}})^3\left[0.791\left(\frac{\tilde{\rho}g}{h_v}\right)+B_{\text{flank}}\left(\frac{\sigma}{h^3}\right)\right]\right\}^{1/4} \tag{2}$$

where $\overline{\Delta T}_{\text{flank}}$ is a mean temperature difference between the vapour and the fin flank, B_{flank} is a dimensionless constant, and h_v is the 'mean vertical fin height', given by

$$h_v = \frac{\phi_f}{\sin(\phi_f)}h, \qquad \phi_f \leqslant \frac{\pi}{2} \tag{3a}$$

$$h_v = \frac{\phi_f}{2-\sin(\phi_f)}h, \quad \frac{\pi}{2} < \phi_f \leqslant \pi \tag{3b}$$

where ϕ_f is the angular position, measured from the top of the tube, below which the interfin space is completely filled with retained condensate.

For the interfin space

$$q_{\text{int}} = B_1\left\{\frac{\rho h_{\text{fg}}}{\mu}(k\Delta T_{\text{int}})^3\left[(\xi(\phi_f))^3\left(\frac{\tilde{\rho}g}{d}\right)+B_{\text{int}}\left(\frac{\sigma}{s^3}\right)\right]\right\}^{1/4} \tag{4}$$

where B_1 and B_{int} are dimensionless constants and $\xi(\phi)$ results from application of the Nusselt [3] analysis for a horizontal tube above the level of condensate retention, and can be closely approximated by

$$\xi(\phi) = 0.874+0.1991\times10^{-2}\phi-0.2642\times10^{-1}\phi^2 +0.5530\times10^{-2}\phi^3-0.1363\times10^{-2}\phi^4. \tag{5}$$

ϕ_f is given, for rectangular-section fins, by the expression of Honda *et al.* [4]

NOMENCLATURE

B_{flank}	dimensionless constant in equation (2)
B_{int}	dimensionless constant in equation (4)
B_{tip}	dimensionless constant in equation (1)
B_1	dimensionless constant in equation (4)
d	diameter of plain tube or fin root diameter of finned tube
d_0	diameter at fin tip
f_f	fraction of fin flank above ϕ_f blanked by retained condensate
f_s	fraction of interfin tube surface blanked by retained condensate
g	specific force of gravity
h	fin height
h_{fg}	specific enthalpy of evaporation
h_v	mean vertical fin height, see equations (3)
k	thermal conductivity of condensate
k_w	thermal conductivity of fin
m	$\sqrt{(2\alpha_{flank}/k_w t)}$
Q_{fin}	heat-transfer rate to fin
Q_{flood}	heat-transfer rate to 'flooded' part of tube
Q_{int}	heat-transfer rate to interfin space in 'unflooded' part of tube
Q_{plain}	heat-transfer rate to plain tube over length equal to one fin pitch of finned tube
q	heat flux
q_{flank}	heat flux to fin flank in 'unflooded' part of tube
q_{int}	heat flux to interfin space in 'unflooded' part of tube
q_{plain}	heat flux to plain tube
q_{tip}	heat flux to fin tip
$q_{tip,flood}$	heat flux to fin tip in 'flooded' part of tube
s	spacing between rectangular-section fins
T_{int}	tube surface temperature in interfin space
T_{root}	fin-root temperature (equal to T_{int})
$T_{tip,flood}$	fin-tip temperature in flooded region
T_v	vapour temperature
t	fin thickness
x	coordinate radially outward along fin flank, with $x = 0$ at fin root.

Greek symbols

α	vapour-side, heat-transfer coefficient, $q/\Delta T$
α_{flank}	mean heat-transfer coefficient for unflooded part of fin flank
α_{tip}	heat-transfer coefficient for fin tip over unflooded part of tube
ΔT	vapour-side temperature difference
ΔT_{flank}	local vapour-side temperature difference on fin flank
$\overline{\Delta T}_{flank}$	average vapour-side temperature difference on fin flank, defined by equation (10)
ΔT_{int}	vapour-side temperature difference in interfin space
ΔT_{tip}	vapour-side temperature difference at fin tip
$\Delta T_{tip,flood}$	vapour-side temperature difference at fin tip in flooded region
$\varepsilon_{\Delta T}$	enhancement ratio (heat-transfer coefficient for finned tube divided by heat-transfer coefficient for plain tube, both based on plain tube area at fin root diameter and for same vapour-side temperature difference)
μ	viscosity of condensate
$\xi(\phi)$	function given by equation (5)
ρ	density of condensate
ρ_v	density of vapour
$\tilde{\rho}$	$\rho - \rho_v$
σ	surface tension
ϕ	angle measured from top of tube
ϕ_f	retention angle, measured from top of tube to the position at which interfin space becomes full of condensate.

$$\phi_f = \cos^{-1}\left\{\frac{4\sigma}{\rho g s d_0} - 1\right\}. \tag{6}$$

When the surface temperature of the fin is taken to be constant and equal to the temperature of the tube at the fin root (as in refs. [1, 2] and valid when $(\alpha h^2/tk_w)$ is small) we have

$$\Delta T_{tip} = \overline{\Delta T}_{flank} = \Delta T_{int} = \Delta T. \tag{7}$$

With this assumption, equations (1), (2) and (4) can be combined, along with the relevant surface areas and the Nusselt [3] equation for condensation on a plain tube, to produce the following equation for the enhancement ratio of a finned tube (defined as the heat-transfer coefficient of the finned tube, based on a plain-tube area of fin root diameter, d, divided by that of a plain tube having diameter d, and for the same vapour-side temperature difference)

$$\varepsilon_{\Delta T} = \left(\frac{d_0}{d}\right)^{3/4} t\left\{0.281 + \frac{B_{tip}\sigma d_0}{t^3\tilde{\rho}g}\right\}^{1/4} + \frac{\phi_f}{\pi}\left[(1-f_f)\frac{d_0^2-d^2}{2h_v^{1/4}d^{3/4}}\left\{0.791 + \frac{B_{flank}\sigma h_v}{h^3\tilde{\rho}g}\right\}^{1/4} + B_1(1-f_s)s\left\{(\xi(\phi_f))^3 + \frac{B_{root}\sigma d}{s^3\tilde{\rho}g}\right\}^{1/4}\right]\Big/ 0.728(s+t) \tag{8}$$

where f_f and f_s are the proportions of fin flank and interfin space, respectively, above the flooding angle ϕ_f, covered by retained wedges of condensate in the fin root corners. As shown in ref. [5], f_f and f_s can be approximated by

$$f_f = (2\sigma/\rho g d h)(\tan(\phi_f/2)/\phi_f) \quad (9a)$$

$$f_s = (4\sigma/\rho g d s)(\tan(\phi_f/2)/\phi_f). \quad (9b)$$

Note that equation (8) involves only geometric parameters and the property ratio $\sigma/\tilde{\rho}$.

Rose [1, 2] found that, with $B_{tip} = B_{flank} = B_{int} = 0.143$ and $B_1 = 2.96$, equation (8) represented most of the available experimental data for condensation on copper tubes to better than 20% and gave the correct dependence on fin spacing, thickness and height.

When the parameter $(\alpha h^2/tk_w)$ becomes large, conduction in the fin can no longer be neglected. In view of the approximations used in the original model [1, 2] it was deemed adequate to include the effect of temperature variation along the fin in an approximate and readily usable way. This was done by dividing the tube into flooded and unflooded parts. In the flooded part the fin flanks were assumed adiabatic, giving a linear temperature variation along the fin, while in the unflooded part an average value of the flank temperaturem, and hence of the vapour-to-flank temperature difference $\overline{\Delta T}_{flank}$, in equation (2), with $\overline{\Delta T}_{flank}$ given by

$$\overline{\Delta T}_{flank} = \frac{1}{h}\int_0^h \Delta T(x)\,dx. \quad (10)$$

Then

$$\Delta T_{tip} < \overline{\Delta T}_{flank} < \Delta T_{int} \quad (11)$$

and for given values of T_v and T_{int} $(=T_{root})$ we have a sufficient number of equations to determine q_{tip}, q_{flank}, ΔT_{tip} and $\overline{\Delta T}_{flank}$ for the unflooded part of the tube.

In the flooded part of the tube, equation (1) gives the heat flux at the fin tip as a function of fin geometry, fluid properties and the fin tip temperature difference, $\Delta T_{tip,flood}$. Assuming that, in the flooded region, the fin flanks are adiabatic ($k \ll k_w$) and neglecting change in cross-section with height (low fins) gives

$$q_{tip,flood} = \frac{k_w(T_{tip,flood} - T_{root})}{h} \quad (12)$$

where $T_{tip,flood} = T_v - \Delta T_{tip,flood}$.

Writing $\Delta T_{tip,flood}$ for ΔT_{tip} in equation (1) and equating the right-hand sides of equations (1) and (12) results in an equation for $\Delta T_{tip,flood}$ which can be solved for given values of T_v and T_{root}, and hence $q_{tip,flood}$ can be found from either equation (1) or (12). The total heat-transfer rate to the flooded region for one fin pitch can then be found from,

$$Q_{flood} = (\pi - \phi_f)d_0 t q_{tip,flood}. \quad (13)$$

In the unflooded region we again have expressions for the heat flux to the fin tip, flank and root as functions of geometry, fluid properties and the fin tip, flank or root temperature differences, respectively (equations (1), (2) and (4)). For the interfin space, ΔT_{int} $(=T_v - T_{int})$ is known for given values of T_v and T_{root}, and q_{int} can be calculated directly using equation (4). The heat-transfer rate to one interfin space is given by

$$Q_{int} = \phi_f(1-f_s)dsq_{int}. \quad (14)$$

For the fin, the problem is complicated by the fact that the temperature at the fin flank, and hence ΔT_{flank}, varies with distance from the fin root. As mentioned above we here adopt a mean value, defined by equation (10), for the vapour-to-flank temperature difference $\overline{\Delta T}_{flank}$ in equation (2).

Thus

$$\alpha_{flank} = \frac{q_{flank}}{\overline{\Delta T}_{flank}} = \left\{\frac{\rho h_{fg}k^3}{\mu\overline{\Delta T}_{flank}}\left[0.791\left(\frac{\tilde{\rho}g}{h_v}\right) + B_{flank}\left(\frac{\sigma}{h^3}\right)\right]\right\}^{1/4}. \quad (15)$$

From equation (1), α_{tip} is given by

$$\alpha_{tip} = \frac{q_{tip}}{\Delta T_{tip}} = \left\{\frac{\rho h_{fg}k^3}{\mu\Delta T_{tip}}\left[0.281\left(\frac{\tilde{\rho}g}{d_0}\right) + B_{tip}\left(\frac{\sigma}{t^3}\right)\right]\right\}^{1/4}. \quad (16)$$

For low fins we neglect changes in cross-section; the 'slender-fin' approximation for the conduction problem then gives, for the local vapour-to-surface temperature difference along the fin

$$\frac{\Delta T(x)}{\Delta T} = \frac{\cosh[m(h-x)] + (\alpha_{tip}/mk_w)\sinh[m(h-x)]}{\cosh(mh) + (\alpha_{tip}/mk_w)\sinh(mh)} \quad (17)$$

where

$$m = \sqrt{\left(\frac{2\alpha_{flank}}{k_w t}\right)}. \quad (18)$$

From equation (17)

$$\Delta T_{tip} = \Delta T(h) = \frac{\Delta T}{\cosh(mh) + (\alpha_{tip}/mk_w)\sinh(mh)} \quad (19)$$

and

$$\overline{\Delta T}_{flank} = \frac{\Delta T}{mh}\left[\frac{\sinh(mh) + (\alpha_{tip}/mk_w)\{\cosh(mh) - 1\}}{\cosh(mh) + (\alpha_{tip}/mk_w)\sinh(mh)}\right]. \quad (20)$$

Substitution for α_{flank} from equation (15) and α_{tip} from equation (16) into equations (19) and (20) leaves two equations with two unknowns, i.e. $\overline{\Delta T}_{flank}$ and ΔT_{tip}, which may be solved by iteration for given values of T_v and T_{root}. q_{tip} and q_{flank} can then be found from equations (1) and (2), respectively.

The total heat-transfer rate to one fin in the unflooded region is then given by

$$Q_{fin} = \phi_f \left\{ d_0 t q_{tip} + (1-f_f)\frac{(d_0^2-d^2)}{2} q_{flank} \right\}. \quad (21)$$

For a plain tube with fin root diameter, the Nusselt [3] theory gives

$$q_{plain} = 0.728 \left\{ \frac{\rho\tilde{\rho} g k^3 h_{fg} \Delta T^3}{\mu d} \right\}^{1/4}. \quad (22)$$

So that the heat-transfer rate over a length equal to one fin pitch is

$$Q_{plain} = \pi d(s+t) q_{plain}. \quad (23)$$

The enhancement ratio, $\varepsilon_{\Delta T}$, is then given by

$$\varepsilon_{\Delta T} = \frac{Q_{flood} + Q_{fin} + Q_{int}}{Q_{plain}} \quad (24)$$

where Q_{flood}, Q_{int}, Q_{fin} and Q_{plain} are obtained from equations (13), (14), (21) and (23), respectively.

RESULTS

Calculations have been made for steam and CFC11 using typical fin and tube dimensions and for thermal conductivities ranging from 80 W m^{-1} K^{-1} (bronze) to 400 W m^{-1} K^{-1} (copper). It was verified that when using a very large value of fin thermal conductivity, the procedure outlined above led to the same results as in refs. [1, 2] where temperature drop along the fin was neglected. In the unmodified theory the enhancement ratio was independent of vapour-side temperature difference. The extent to which the present modification leads to a dependence on vapour-side temperature difference was investigated and found to be very small. For steam at 100°C and CFC11 at 60°C, the enhancement ratio was virtually independent of vapour-side temperature difference for all thermal conductivities and geometries used, falling off slightly at low values of vapour-side temperature difference (around 5 K for steam and 1 K for CFC11).

The effect of fin spacing was studied for steam and CFC11 and for fin thermal conductivities in the range 80–400 W m^{-1} K^{-1}. The optimum spacing (that giving highest vapour-side enhancement ratio) was found to be almost independent of tube thermal conductivity, fin height and fin thickness, and not strongly dependent on fin-root diameter in the range 10–30 mm. For CFC11 the optimum fin spacing was between 0.25 and 0.35 mm, with larger diameter tubes having larger optimum fin spacing. For steam, the optimum fin spacing was between 1 and 1.5 mm, the peak being much less sharp than in the case of the refrigerant so that in practice the choice of fin spacing would be less critical in the case of steam. These general conclusions are the same as those given by the unmodified theory [1, 2]; the effect of thermal conductivity therefore has little effect on the optimum spacing between fins.

Effect of fin height was studied using various fin thicknesses in the practical range, with near-optimum values of fin spacing for steam (1.25 mm) and CFC11 (0.3 mm). The results, for a fin root diameter of 12.7 mm, are shown in Fig. 1. It is seen that the increase in enhancement ratio with fin height is almost linear in all cases. For CFC11 the effect of fin thermal conductivity is relatively weak and the enhancement ratio continues to increase significantly with fin height in the practical range. For steam, with much higher heat-transfer coefficients on the fin surfaces, the effect of fin thermal conductivity is stronger as expected. For the lower thermal conductivity materials, there is evidently no advantage in increasing the fin height.

Figure 2 shows the calculated variation of enhancement ratio with fin thickness for the same fluids and fin thermal conductivities with near-optimum fin spacing and for a fin height of 1 mm. For both fluids it may be seen that the optimum fin thickness increases as the fin thermal conductivity decreases. For CFC11

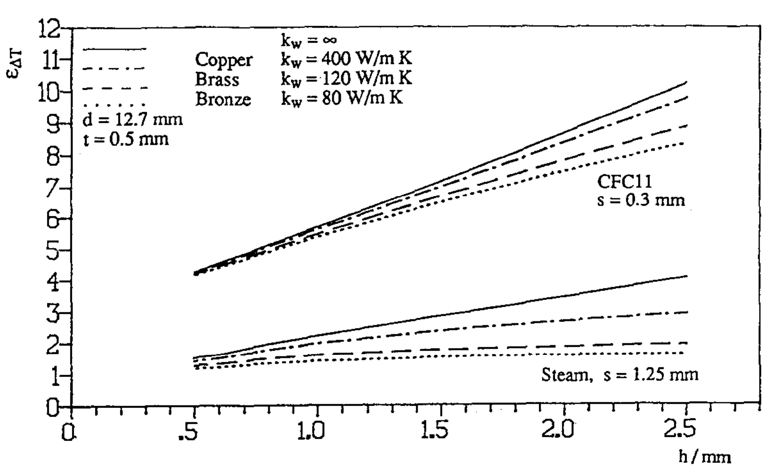

FIG. 1. Variation of predicted vapour-side enhancement ratio with fin height.

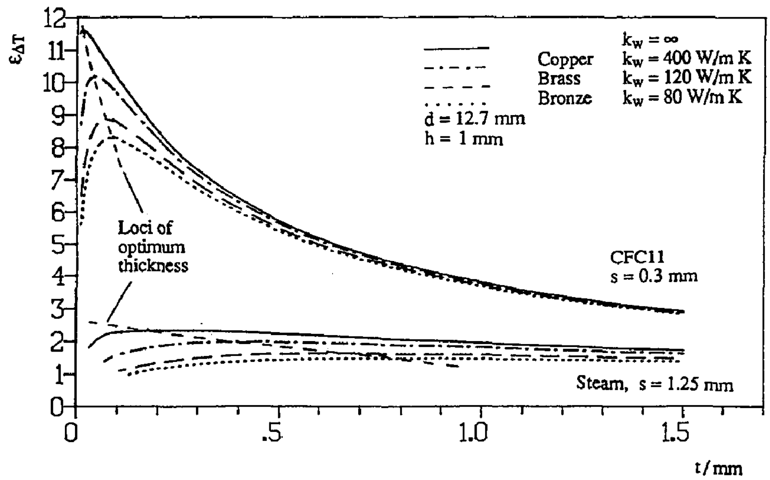

Fig. 2. Variation of predicted vapour-side enhancement ratio with fin thickness.

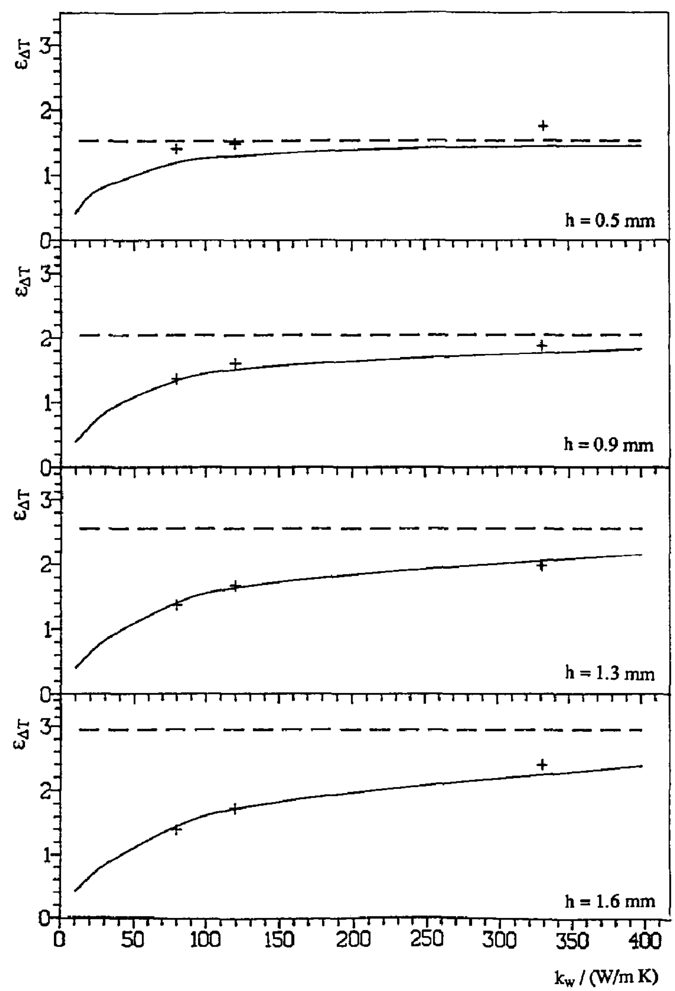

Fig. 3. Variation of vapour-side enhancement ratio with fin thermal conductivity; comparison with experimental data [6] for steam ($T_v = 100°C$, $\Delta T = 20$ K, $d = 12.7$ mm, $t = 0.5$ mm, $s = 1$ mm - - - - - [1, 2], $k_w = \infty$, ——— present model, + [6]).

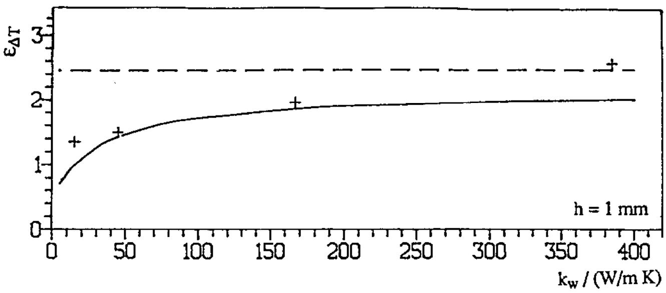

FIG. 4. Variation of vapour-side enhancement ratio with fin thermal conductivity; comparison with experimental data [7] for steam ($T_v = 100°C$, $\Delta T = 30$ K, $d = 13.9$ mm, $t = 1$ mm, $s = 1.5$ mm - - - - [1, 2], $k_w = \infty$, ——— present model, + [7]).

the peaks in enhancement ratio are at fin thicknesses of 0.05, 0.07 and 0.09 mm for copper, brass and bronze, respectively. For larger fin thickness, the enhancement ratio drops off quite steeply and the effect of fin thermal conductivity on enhancement ratio diminishes. Similar results are obtained for steam except that the curves are much flatter with peaks at fin thicknesses of 0.4, 0.7 and 0.8 mm for copper, brass and bronze, respectively.

It is evident from Figs. 1 and 2 that for steam there is little or no advantage in using finned tubes for the lower conductivity materials.

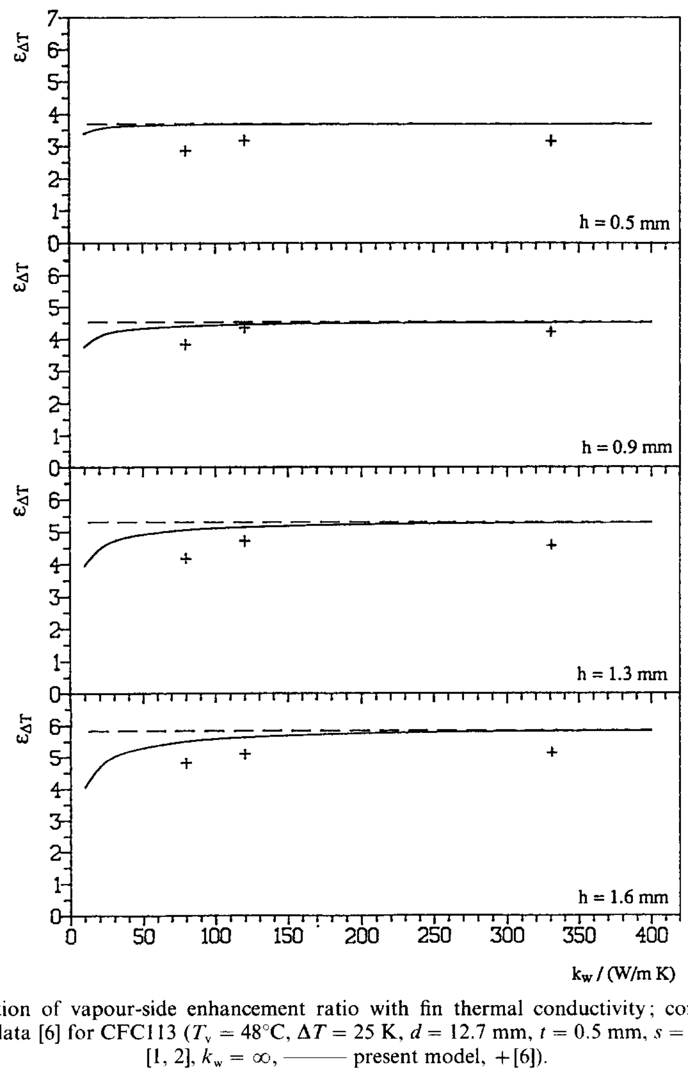

FIG. 5. Variation of vapour-side enhancement ratio with fin thermal conductivity; comparison with experimental data [6] for CFC113 ($T_v = 48°C$, $\Delta T = 25$ K, $d = 12.7$ mm, $t = 0.5$ mm, $s = 1$ mm - - - - [1, 2], $k_w = \infty$, ——— present model, + [6]).

COMPARISON WITH EXPERIMENTAL DATA

Huang *et al.* [6] have recently done tests with CFC113 and steam condensing on copper, brass and bronze finned tubes. Four tubes of each material were tested, with constant fin root diameter, fin thickness and fin spacing of 12.7, 0.5 and 1.0 mm, respectively, and fin heights of 0.5, 0.9, 1.3 and 1.6 mm. The thermal conductivity of the three materials, calculated from the measured electrical conductivity, were found to be around 80, 120 and 330 W m^{-1} K^{-1} for bronze, brass and copper tubes, respectively, over the range of temperatures of interest. Data on the effect of thermal conductivity have also been obtained recently by Cobb [7], who condensed steam on tubes of stainless steel, aluminium, copper-nickel alloy and copper (quoted thermal conductivities of 15, 30, 75 and 400 W m^{-1} K^{-1}, respectively) with constant fin root diameter of 13.7 mm, and constant film thickness, spacing and height of 1.0, 1.5 and 1.0 mm, respectively.

Figures 3 and 4 compare the steam data from refs. [6, 7], respectively, with theory, on the basis of enhancement ratio against tube thermal conductivity. The theory shows good general agreement with the experimental data, and correctly identifies the general dependence on fin thermal conductivity.

The CFC113 data of Huang *et al.* [6] are compared to theory in Fig. 5. For all tube materials and fin geometries tested theory and experiment agree to within about 15%, and both show that for tubes with thermal conductivity above about 50 W m^{-1} K^{-1}, enhancement ratio is essentially independent of tube material.

Also shown on Figs. 3–5 are results of the earlier model [1, 2]. It can be seen that in all cases, the present model approaches that of refs. [1, 2] as fin thermal conductivity becomes large.

CONCLUSIONS

The model of Rose [1, 2] for condensation on horizontal, integral-fin tubes has been adapted to account for 'fin efficiency' effects. The modified model should, in principle, be able to predict optimum fin thickness, spacing and height for a given fluid and tube diameter. In practice, the optimum fin height was outside the range of the low fin approximation used in the model. The best fin spacing was essentially independent of other geometric variables and fin thermal conductivity. The best fin thickness was strongly dependent on fin thermal conductivity and fluid. For the refrigerant the optimum fin thickness is smaller than presently used in practice.

REFERENCES

1. J. W. Rose, Condensation on low-finned tubes—an equation for vapor-side enhancement, *Proc. Engineering Foundation Conf.—Condensation and Condenser Design*, St. Augustine, Florida, ASME, pp. 317–333 (1994).
2. J. W. Rose, An approximate equation for the vapour-side heat-transfer coefficient for condensation on low-finned tubes, *Int. J. Heat Mass Transfer* **37**, 865–875 (1994).
3. W. Nusselt, Die Oberflachenkondensation des Wasserdampfes, *Z. Vereines Deutsch. Ing.* **60**, 541–546, 569–575 (1916).
4. H. Honda, S. Nozu and K. Mitsumori, Augmentation of condensation on horizontal finned tubes by attaching a porous drainage plate, *Proc. ASME–JSME Thermal Engng Joint Conf.*, Vol. 3, pp. 289–296 (1983).
5. H. Masuda and J. W. Rose, Static configuration of liquid films on horizontal tubes with low radial fins: implications for condensation heat transfer, *Proc. Roy. Soc. Lond.* **A410,** 125–139 (1987).
6. X.-S. Huang, A. Briggs and J. W. Rose, Effect of thermal conductivity of tube material on condensation heat transfer on integral-fin tubes, *Proc. 10th Int. Heat Transfer Conf.*, Brighton (in press).
7. R. Cobb, The influence of wall conductivity on film condensation with integral fin tubes. M.Sc. Thesis, Naval Postgraduate School, Monterey, California (1993).